

Provided for non-commercial research and education use.  
Not for reproduction, distribution or commercial use.



This article appeared in a journal published by Elsevier. The attached copy is furnished to the author for internal non-commercial research and education use, including for instruction at the authors institution and sharing with colleagues.

Other uses, including reproduction and distribution, or selling or licensing copies, or posting to personal, institutional or third party websites are prohibited.

In most cases authors are permitted to post their version of the article (e.g. in Word or Tex form) to their personal website or institutional repository. Authors requiring further information regarding Elsevier's archiving and manuscript policies are encouraged to visit:

<http://www.elsevier.com/copyright>



Contents lists available at ScienceDirect

## DNA Repair

journal homepage: [www.elsevier.com/locate/dnarepair](http://www.elsevier.com/locate/dnarepair)

## Repair activities of human 8-oxoguanine DNA glycosylase are stimulated by the interaction with human checkpoint sensor Rad9–Rad1–Hus1 complex

Min Ju Park<sup>a,1</sup>, Jong-Hwa Park<sup>b,1</sup>, Soo-Hyun Hahm<sup>a</sup>, Sung Il Ko<sup>a</sup>, You Ri Lee<sup>a</sup>, Ji Hyung Chung<sup>c</sup>, Sun Young Sohn<sup>d,e</sup>, Yunje Cho<sup>d,e</sup>, Lin-Woo Kang<sup>a</sup>, Ye Sun Han<sup>a,\*</sup>

<sup>a</sup> Department of Advanced Technology Fusion, Konkuk University, Hwayang-dong, Gwangjin-gu, Seoul 143-701, Republic of Korea

<sup>b</sup> Bio/Molecular Informatics Center, Konkuk University, Hwayang-dong, Gwangjin-gu, Seoul 143-701, Republic of Korea

<sup>c</sup> Yonsei Integrative Research Institute for Cerebral & Cardiovascular Diseases (YIRIC), Yonsei University Health System, Seoul 120-752, Republic of Korea

<sup>d</sup> National Creative Research Center for Structural Biology, Pohang University of Science and Technology, Pohang 790-784, Republic of Korea

<sup>e</sup> Department of Life Science, Pohang University of Science and Technology, Pohang 790-784, Republic of Korea

## ARTICLE INFO

## Article history:

Received 23 January 2009

Received in revised form 15 May 2009

Accepted 16 June 2009

Available online 16 July 2009

## Keywords:

Human 8-oxoguanine DNA glycosylase  
Human Rad9–Rad1–Hus1 (9–1–1) complex  
8-Oxoguanine  
Excision activity  
Trapping assay

## ABSTRACT

Rad9–Rad1–Hus1 (9–1–1) is a checkpoint protein complex playing roles in DNA damage sensing, cell cycle arrest, DNA repair or apoptosis. Human 8-oxoguanine DNA glycosylase (hOGG1) is the major DNA glycosylase responsible for repairing a specific aberrantly oxidized nucleotide, 7,8-dihydro-8-oxoguanine (8-oxoG). In this study, we identified a novel interaction between hOGG1 and human 9–1–1, and investigated the functional consequences of this interaction. Co-immunoprecipitation assays using transiently transfected HEK293 cells demonstrated an interaction between hOGG1 and the 9–1–1 proteins. Subsequently, GST pull-down assays using bacterially expressed and purified hOGG1-His and GST-fused 9–1–1 subunits (GST-hRad9, GST-hRad1, and GST-hHus1) demonstrated that hOGG1 interacted directly with the individual subunits of the human 9–1–1 complex. *In vitro* excision assay, which employed a DNA duplex containing an 8-oxoG/C mismatch, showed that hRad9, hRad1, and hHus1 enhanced the 8-oxoG excision and  $\beta$ -elimination activities of hOGG1. In addition, the presence of hRad9, hRad1, and hHus1 enhanced the formation of covalently cross-linked hOGG1–8-oxoG/C duplex complexes, as determined by a trapping assay using NaBH<sub>4</sub>. A trimeric human 9–1–1 complex was purified from *Escherichia coli* cell transformed with hRad9, His-fused hRad1, or His-fused hHus1 expressing vectors. It also showed the similar activity to enhance *in vitro* hOGG1 glycosylase activity, compared with individual human 9–1–1 subunits. Detection of 8-oxoG in HEK293 cells using flow cytometric and spectrofluorometric analysis revealed that over-expression of hOGG1 or human 9–1–1 reduced the formation of 8-oxoG residues following the H<sub>2</sub>O<sub>2</sub> treatment. The highest 8-oxoG reduction was observed in HEK293 cells over-expressing hOGG1 and all the three subunits of human 9–1–1. These indicate that individual human 9–1–1 subunits and human 9–1–1 complex showed almost the same abilities to enhance the *in vitro* 8-oxoG excision activity of hOGG1, but that the greatest effect to remove 8-oxoG residues in H<sub>2</sub>O<sub>2</sub>-treated cells was derived from the 9–1–1 complex as a whole.

© 2009 Elsevier B.V. All rights reserved.

### 1. Introduction

Reactive oxygen species (ROS) are generated during normal cellular respiration or because of exposure to certain environmental agents. ROS induce DNA damage that involves several oxidized base modifications within free nucleotides or DNA strands [1,2]. Such DNA damage may cause loss of both genomic integrity and aging-associated cellular regulation; it is also associated with a variety of diseases, including cancer [3,4]. A stable oxidized form of guanine,

7,8-dihydroxy-8-oxoguanine (8-oxoguanine, 8-oxoG), is the most abundant product of ROS-induced DNA lesion and is a key indicator of cellular oxidative stress [5,6]. All organisms utilize DNA base excision repair (BER) pathways to repair oxidatively induced DNA lesions, including 8-oxoG [7,8]. BER is mediated by specific DNA glycosylases that recognize and hydrolyze the modified base [7,9,10]. Human 8-oxoguanine DNA glycosylase (hOGG1) is a representative BER DNA glycosylase that removes mutagenic 8-oxoG lesions situated opposite cytosines and generates apurinic/apyrimidinic (AP) sites [11–13]. Although hOGG1 utilizes its AP-lyase activity ( $\beta$ -elimination) to cleave the strand 3' to the AP site [14], hOGG1 does not effectively catalyze strand cleavage; its AP-lyase activity is significantly lower than its glycosylase activity. Instead, AP endonuclease I (APE1, or ref-1) recognizes the AP site and cleaves the DNA

\* Corresponding author. Tel.: +82 2 2049 6050; fax: +82 2 452 3410.

E-mail address: [yshan@konkuk.ac.kr](mailto:yshan@konkuk.ac.kr) (Y.S. Han).

<sup>1</sup> These authors contributed equally to this work.

backbone 5' to the AP site, generating a 3' hydroxyl group and a 5' phosphate group [15].

Human Rad9–Rad1–Hus1 (9–1–1) complex, a heterotrimeric complex that is structurally homologous to the homotrimeric proliferating cell nuclear antigen (PCNA), plays a key role in checkpoint activation [16,17] and functions as a DNA damage sensor. The 9–1–1 subunits form a DNA damage-responsive complex that clamps around the damaged DNA and transduces the damage signal to downstream effectors. Replication stress or other types of DNA damage result in phosphorylation and activation of checkpoint kinase 1 (Chk1) through ataxia telangiectasia and Rad3-related protein (ATR) [18]. Activated Chk1 plays a critical role in cellular checkpoint responses by stabilizing stalled replication forks, blocking the firing of late origin of replication forks, and arresting cells at G2/M phase. The human 9–1–1 complex is a key participant in the ATR-dependent signaling pathway that mediates Chk1 activation. Together, these proteins play a critical role in facilitating DNA replication and maintaining genomic integrity [19]. Recent work suggested that the human 9–1–1 complex interacts with the BRCT I–II region of TopBP1. This interaction induces the TopBP1 activation domain to bind and activate ATR, thus mediating Chk1 phosphorylation by ATR [20,21].

The 9–1–1 complex also functions as a collaborator to enhance the repair activity of BER proteins. Specifically, the 9–1–1 complex directly interacts with and stimulates the activation of the BER-related proteins APE1, flap endonuclease I (FEN1), polymerase  $\beta$ , and DNA ligase I [22–26]. Additionally, the human 9–1–1 complex physically and functionally interacts with DNA glycosylases such as MutY homolog (MYH), Nei-like glycosylase I (NEIL1), and thymine DNA glycosylase (TDG) [27–30].

To our knowledge, this work is the first to report that hRad9, hRad1, and hHus1 physically and functionally interacted with hOGG1, and that these interactions increased the catalytic activity of hOGG1 by enhancing its DNA binding activity. In addition, HEK293 cells transiently over-expressing hOGG1 or human 9–1–1 dramatically reduced the levels of H<sub>2</sub>O<sub>2</sub>-induced 8-oxoG residues.

## 2. Materials and methods

### 2.1. Cell lines

Human embryonic kidney HEK293 cells were grown in Dulbecco's modified Eagle's medium (DMEM; Invitrogen, Carlsbad, CA) supplemented with 10% FBS (Invitrogen) and 1% penicillin–streptomycin solution (Sigma, St. Louis, MO) at 37 °C in a 5% CO<sub>2</sub> incubator. HEK293 cells were seeded onto 6-well plates at a density of  $1 \times 10^6$  cells per well and incubated for 24 h before experiments. *Escherichia coli* strain BL21 (DE3) was used as a host for cloning and purification of recombinant proteins.

### 2.2. Expression plasmid construction

Gene fragments corresponding to the coding regions of hOGG1, hRad9, hRad1, and hHus1 (accession numbers: hOGG1, NM016821; hRad9, NM004584; hRad1, NM002853; hHus1, NM004507) were amplified using PCR. The hOGG1 fragment was sub-cloned into pCMV Tag3A using *EcoRI* and *Sall* sites (Stratagene, La Jolla, CA); hRad9, hRad1, and hHus1 fragments were sub-cloned into pCMV Tag2C using *BamHI* and *Sall* sites (Stratagene). To facilitate expression and purification of the recombinant hOGG1, hRad9, hRad1, and hHus1 proteins, C-terminal polyhistidine-tagged DNA fragments were generated from the pCMV Tag3A/hOGG1 or pCMV Tag2C containing hRad9, hRad1, or hHus1 constructs using PCR. These tagged constructs were then sub-cloned into the pGEX4T-1 bacterial expression vector (GE Healthcare, Princeton, NJ).

Also, polyhistidine-untagged hRad9 (hRad9), polyhistidine-tagged hRad9 (His-hRad9), polyhistidine-tagged hRad1 (His-hRad1), and polyhistidine-tagged hHus1 (His-hHus1) fragments were sub-cloned into pET-28a (EMD Chemicals Inc., San Diego, CA) or modified pET-28a expression vectors containing different antibiotics (ampicillin, streptomycin, or chloramphenicol) resistance genes. The identities of all constructs were confirmed by both restriction enzyme mapping and DNA sequence analyses.

### 2.3. Transient expression of hOGG1, hRad9, hRad1, and hHus1

Expression vectors were transiently transfected into 80–90% confluent HEK293 cells in 6-well plates or 100 cm<sup>2</sup> dishes using Lipofectamine™ 2000 reagent (Invitrogen) according to the manufacturer's protocol. After a 36 h incubation, cells were lysed in lysis buffer [50 mM Tris–HCl (pH 8.0), 100 mM NaCl, 5 mM EDTA, 1 mM NaF, 1 mM Na<sub>3</sub>VO<sub>4</sub>, 1% Nonidet P-40, 10  $\mu$ g/ml PMSF, protease inhibitor cocktail (Sigma)] for 1 h at 4 °C with occasional vortexing. After centrifugation, supernatants were collected and used in the Western blot analysis and immunoprecipitation experiments described below.

### 2.4. Co-immunoprecipitation

Total cell lysates were collected from the HEK293 cells transfected with different sets of expression vectors and pre-cleared with 30  $\mu$ l protein G–Sepharose beads (Santa Cruz Biotech., Santa Cruz, CA) to remove nonspecific proteins. After 1 h incubation, cell lysates were separated from the beads by centrifugation. Pre-cleared supernatants were incubated for 3 h with 2  $\mu$ g of anti-c-myc (Santa Cruz Biotech.) followed by 12 h incubation with 30  $\mu$ l of protein A/G–Sepharose beads, all at 4 °C under gentle rotation. Protein–bead complexes were precipitated by centrifugation at 600  $\times$  g for 5 min, washed five times with washing buffer (1:1 mixture of lysis buffer and PBS), and mixed with 2  $\times$  SDS polyacrylamide gel loading buffer. After boiling for 5 min, immunoprecipitated samples were resolved on SDS polyacrylamide gel and subjected to Western blot analysis.

### 2.5. Expression and purification of hOGG1, GST-fused hRad9, hRad1 and hHus1

*E. coli* cells harboring the expression vectors described above (pGEX4T-1/hOGG1-His, pGEX4T-1/hRad9-His, pGEX4T-1/hRad1-His, or pGEX4T-1/hHus1-His) were cultured in LB medium supplemented with 50  $\mu$ g/ml ampicillin. When cells reached an A<sub>600</sub> of 0.6, protein expression was induced by adding isopropylthiogalactoside (IPTG, final concentration of 0.2 mM) to the cells and incubating for 16 h at 18 °C. Cells were harvested, resuspended in PBS (pH 7.4), and lysed by ultrasonication. Following centrifugation at 16,000  $\times$  g for 30 min, the supernatant was applied to glutathione–Sepharose 4B resin (GE Healthcare) pre-equilibrated with PBS. After washing with five column volumes of PBS, the GST fusion protein of interest (GST-fused hOGG1, hRad9, hRad1, or hHus1) was eluted with a buffer containing 50 mM Tris–HCl (pH 8.0) and 10 mM reduced glutathione. GST-fused hOGG1 was subsequently cleaved with thrombin (10 U/mg of fusion protein) for 16 h at 4 °C, and the resulting protein mixture was applied to a Ni-NTA agarose resin (Qiagen, Valencia, CA) pre-equilibrated with a binding buffer (50 mM NaH<sub>2</sub>PO<sub>4</sub>, 300 mM NaCl, 10 mM imidazole). After washing with five column volumes of binding buffer, proteins bound to the resin were eluted with elution buffers containing different concentrations of imidazole (from 100 to 500 mM). Protein fractions containing GST-fused hRad9, hRad1, or hHus1, partially purified with the glutathione–Sepharose 4B resin as described above, were further purified using the Ni-NTA agarose

resin protocol as described above. Protein purity was verified using SDS-PAGE and Coomassie brilliant blue staining. Purified proteins were dialyzed, concentrated with Vivaspin columns (Vivascience, Germany), and stored at  $-80^{\circ}\text{C}$ . Protein concentrations were determined using the Bio-Rad DC protein assay kit (Bio-Rad, Hercules, CA).

## 2.6. Expression and purification of a trimeric 9–1–1 complex

*E. coli* cell co-transformed with hRad9, His-hRad1 and His-hHus1 expressing vectors was cultured in LB broth medium containing antibiotics (ampicillin, streptomycin and chloramphenicol). Protein expression was induced at an  $A_{600}$  of 0.6 by adding IPTG (a final concentration of 0.2 mM), and the cells were incubated for 16 h at  $18^{\circ}\text{C}$ . The cells were harvested, resuspended in a binding buffer, and lysed by ultrasonication. Following centrifugation at  $16,000 \times g$  for 30 min, the supernatant was applied to a Ni-NTA agarose resin pre-equilibrated with a binding buffer. After washing with five column volumes of binding buffer, proteins bound to the resin were eluted with the elution buffers containing 500 mM imidazole. The fraction was dialyzed, concentrated with Vivaspin column, and applied to a Superdex 200 (10/30GL) column (GE Healthcare) pre-equilibrated with 50 mM phosphate buffer (pH 7.0). Proteins were eluted with the equilibrated buffer at 0.5 ml/min flow rate. The presence of hRad9, His-hRad1, and His-hHus1 in each elute fraction (2.0 ml) was verified using SDS-PAGE and Coomassie brilliant blue staining. Also, His-hRad9, His-hRad1, or His-hHus1 was separately expressed from *E. coli* cells transformed with polyhistidine-tagged hRad9, hRad1, or hHus1 expressing vectors and purified by affinity chromatography using Ni-NTA agarose resin as described above.

## 2.7. GST pull-down assay

Purified hOGG1-His (1  $\mu\text{g}$ ) was mixed with 1  $\mu\text{g}$  purified GST, GST-hRad9, GST-hRad1, or GST-hHus1 in a 1.5-ml microcentrifuge tube containing 300  $\mu\text{l}$  of pre-equilibrated glutathione-Sepharose 4B beads in PBS, followed by incubation for 12 h at  $4^{\circ}\text{C}$  with gentle rotation. Beads were then centrifuged at  $600 \times g$  for 5 min and washed five times with 1 ml of PBS. Proteins bound to the beads were eluted [50 mM Tris-HCl (pH 8.0), 10 mM reduced glutathione] and resolved on a 12% SDS polyacrylamide gel. The proteins were subsequently analyzed by Western blot using anti-His (Santa Cruz Biotech.).

## 2.8. Western blot analysis

Proteins resolved on 8–12% SDS-polyacrylamide gels were transferred onto polyvinylidene difluoride (PVDF) membranes (GE Healthcare). The membranes were blocked overnight at  $4^{\circ}\text{C}$  with 5% nonfat dried milk in TBS-T (TBS with 0.05% Tween-20) and then incubated with anti-c-myc, anti-flag, anti-GST (Sigma), anti-His or anti-hRad9 (Santa Cruz Biotech.), followed by an incubation with appropriate horseradish peroxidase (HRP) conjugated secondary antibodies (Santa Cruz Biotech.). Protein bands were detected using ECL Pico Western blotting detection reagents (Pierce, Rockford, IL).

## 2.9. In vitro hOGG1 excision assay

DNA glycosylase activity was assayed using 39-mer duplex oligonucleotide substrates carrying 8-oxoguanine (8-oxoG) at position 16 [5'-GGA TCC TCT AGA GTC (8-oxoG)AC CTG CAG GCA TGC AAG CTT GAG-3'] and complement oligonucleotides carrying cytosine in the pairing position of 8-oxoG (3'-CCT AGG AGA TCT CAG GTG GAC GTC CGT ACG TTC GAA CTC-5') (Bio-Synthesis

Inc., Lewisville, TX). Oligonucleotides containing 8-oxoG were 5'-end-labeled with T4 polynucleotide kinase (New England Biolabs., Ipswich, MA) in the presence of [ $\gamma$ - $^{32}\text{P}$ ] ATP and purified through a Microspin Sephadex G-50 column (GE Healthcare). Oligonucleotide duplexes were prepared using annealing reactions containing a 1.5-fold molar excess of the unlabeled complementary oligonucleotide. Activity assays were performed in 20  $\mu\text{l}$  reaction volumes with variable concentrations of protein and 1 pmol of the radiolabeled 39-mer oligonucleotide duplex in a reaction buffer [50 mM Tris-HCl (pH 7.5), 100 mM NaCl]. After incubating at  $37^{\circ}\text{C}$  for 1 h, reactions were terminated using  $2\times$  alkaline loading buffer (95% formamide, 10 mM EDTA, 0.05% bromophenol blue) and heated at  $95^{\circ}\text{C}$  for 5 min. Reaction mixtures were resolved by electrophoresis on a denaturing 18% polyacrylamide gel containing 7 M urea in  $1\times$  TBE buffer (90 mM Tris, 90 mM boric acid, 2 mM EDTA). The gel was dried and placed on an imaging plate; DNA cleavage products were quantified using a BAS2000 image analyzer (Fuji, Tokyo, Japan).

## 2.10. hOGG1 trapping assay using $\text{NaBH}_4$

Trapping assay mixtures were assembled in 20  $\mu\text{l}$  volumes with variable combinations of proteins and 1 pmol of the radiolabeled 39-mer oligonucleotide duplex in a reaction buffer [50 mM Tris-HCl (pH 7.5), 100 mM NaCl, 50 mM  $\text{NaBH}_4$ ]. After incubating at  $37^{\circ}\text{C}$  for 30 min, samples were mixed with 5  $\mu\text{l}$  of  $5\times$  SDS polyacrylamide gel loading buffer, boiled at  $95^{\circ}\text{C}$  for 5 min, and separated on a 12% SDS polyacrylamide gel. The gel was dried and placed on an imaging plate; trapped hOGG1-DNA complexes were quantified using a BAS2000 image analyzer.

## 2.11. Immunofluorescence microscopy

To determine the subcellular location of hOGG1 and hRad9, HEK293 cells seeded on polylysine-coated cover slips were transiently transfected with c-myc-hOGG1 expressing vectors (pCMV Tag 3A/hOGG1) for 24 h and treated with 5 mM  $\text{H}_2\text{O}_2$  for 1 h. At room temperature, cells were fixed with 4% paraformaldehyde in PBS for 30 min and permeabilized with 0.25% Triton X-100 in PBS for 30 min. After blocking with 1% BSA in PBS-T (PBS containing 0.5% Tween-20) for 30 min, cells were incubated with Alexa Fluor 647-conjugated mouse anti-c-myc (1:100; AbD Serotec, Oxford, UK) and hRad9 polyclonal antibody (1:100; Santa Cruz Biotech.) for 2 h. The cells were washed three times for 15 min each in PBS and incubated with FITC-conjugated anti-rabbit IgG (1:100; Sigma) for 2 h. Cells were rinsed three times with 1 ml of PBS and viewed with a confocal fluorescence microscope (Olympus FV-1000; software: Olympus Fluoview; Olympus, Center Valley, PA).

## 2.12. Detection of 8-oxoG in cells

*In vivo* 8-oxoG lesions in cells were detected using a fluorescent probe that binds directly to 8-oxoG moieties in the DNA of fixed cells (OxyDNA assay kit; Calbiochem, La Jolla, CA), according to the manufacturer's instructions. HEK293 cells were transfected with hOGG1, hRad9, hRad1, or hHus1 expressing vectors, incubated for 24 h, and treated with 5 mM  $\text{H}_2\text{O}_2$  for 1 h. Cells harvested by trypsinization were washed with PBS, fixed with 2% paraformaldehyde for 15 min on ice, and treated with ice-cold 70% ethanol for 1 h at  $-20^{\circ}\text{C}$ . After several washings with PBS and wash solution, cells were blocked and stained with FITC-conjugated probes (fluorescence probes that bind 8-oxoG residues) for 12 h at  $4^{\circ}\text{C}$  with gentle shaking. Cells were washed five times with wash solution and analyzed with a flow cytometer (FACSCalibur, BD Bioscience, San Jose, CA). Fluorescence emitted from the FITC-conjugated probes was estimated using a minimum of 10,000 cells per sample and analyzed using Cell Quest Alias software (BD Biosciences).

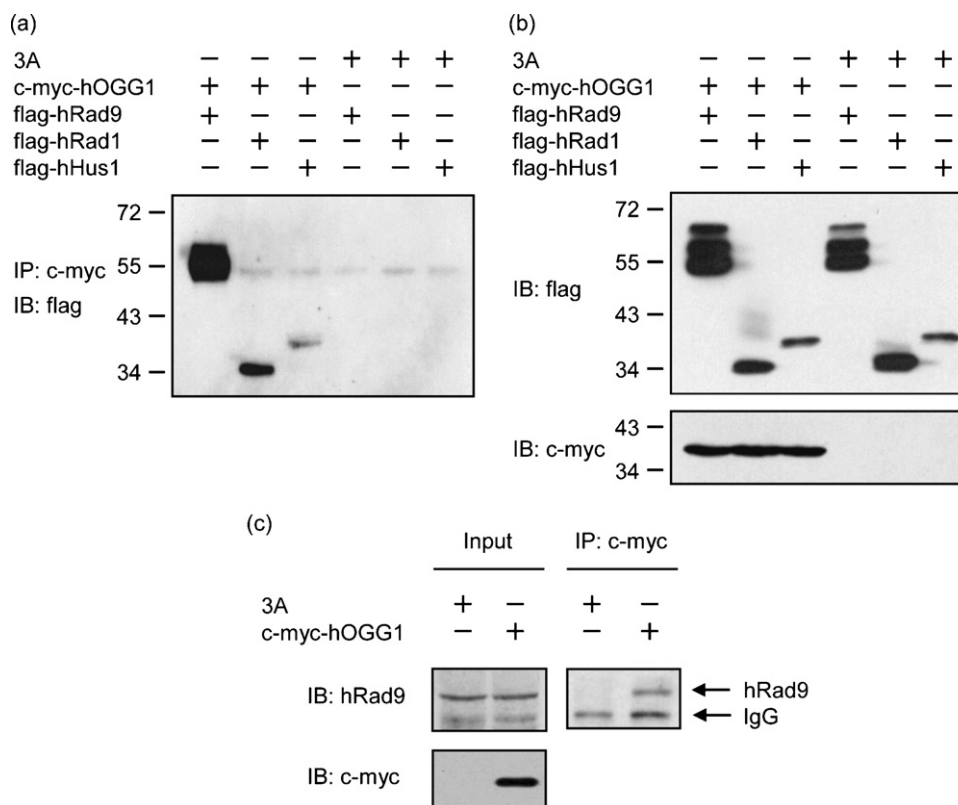


**Fig. 1.** hOGG1 interacted with hRad9, hRad1 and hHus1. (a) Co-immunoprecipitation and Western blot analysis were performed using lysates of HEK293 cells transfected with c-myc-hOGG1, flag-hRad9, flag-hRad1, or flag-hHus1 expressing vector. After co-immunoprecipitation using c-myc antibody, the flag-hRad9, flag-hRad1, and flag-hHus1 that interacted with c-myc-hOGG1 were detected by Western blot analysis using anti-flag. The parental vector pCMV Tag3A (3A) was used as a negative control. (b) Expression levels of each fusion protein in transfected HEK293 cell lysates were detected with Western blot analysis, using anti-c-myc or anti-flag. IP and IB represent immunoprecipitation and immunoblotting, respectively. (c) Co-immunoprecipitation using anti-c-myc was performed with the lysate of HEK293 cell transfected c-myc-hOGG1 expression vector, pCMV Tag3A/hOGG1. The presence of endogenous hRad9 in immunoprecipitates was determined with Western blot analysis using anti-hRad9.

2.13. Statistical analysis

Experiments were performed three times and statistical analysis was conducted using Student's *t*-test. Data are expressed as means  $\pm$  SD and *P* < 0.05 was considered significant.

3. Results

3.1. hOGG1 interacted with hRad9, hRad1, and hHus1

To determine whether hOGG1 interacted with human 9-1-1, we transiently transfected HEK293 cells with expression vectors encoding flag-tagged hRad9, hRad1, hHus1, or c-myc-tagged hOGG1. Interacting proteins were detected by co-immunoprecipitation and Western blot analysis using flag or c-myc antibodies. The hRad1, hHus1, and hOGG1 proteins were expressed as 34-, 38-, and 40-kDa bands, respectively, corresponding to their expected sizes (Fig. 1b). The hRad9 protein was expressed as several bands between 50 and 60 kDa, probably due to post-translational modifications. The human 9-1-1 expression appeared constant regardless of c-myc-hOGG1 expression. Western blot analysis of immunoprecipitated samples using anti-flag showed that flag-hRad9, hRad1 and hHus1 were co-immunoprecipitated with hOGG1 (Fig. 1a). While the flag-hRad1, flag-hHus1, and phosphorylated forms of flag-hRad9 were captured by hOGG1 immunoprecipitation, the co-immunoprecipitation of hyperphosphorylated-hRad9 was not observed. The interaction between hOGG1 and hRad9 was further determined with co-immunoprecipitation of endogenous hRad9 from HEK293 cell extracts being transfected with the c-myc-hOGG1 express-

ing vector, pCMV Tag3A/hOGG1. Endogenous hRad9 was co-immunoprecipitated with anti-c-myc (Fig. 1c). This demonstrates that endogenous hRad9 interacted with the over-expressed c-myc-hOGG1.

We verified the purity of bacterially expressed and purified hOGG1-His, GST, GST-hRad9, GST-hRad1, and GST-hHus1 using SDS-PAGE and Coomassie brilliant blue staining (Fig. 2a and b). We then used the purified proteins in GST pull-down assays to demonstrate physical interactions between hOGG1 and hRad9, hRad1, and hHus1. As shown in Fig. 2c, hOGG1-His was pulled down by GST-hRad9, GST-hRad1, or GST-hHus1, but not GST. The presence of hOGG1 and GST-fused hRad9, hRad1, hHus1 used in GST pull-down assay were determined with Western blot analysis using anti-GST and anti-His (Fig. 2d). Taken together, these results showed that hOGG1 directly interacted with all the three subunits of the human 9-1-1 complex.

3.2. hOGG1 co-localized with hRad9

Since we had demonstrated that the proteins interacted, we next investigated whether they occupied the same subcellular locations during oxidative stress. To conduct these experiments, we treated transiently transfected HEK 293 cells expressing c-myc-hOGG1 with 5 mM H<sub>2</sub>O<sub>2</sub> for 1 h and subjected them to immunofluorescence assays to explore the subcellular distributions of c-myc-hOGG1 and endogenous hRad9. Over-expressed c-myc-hOGG1 appeared in the nucleus of untreated cells (no H<sub>2</sub>O<sub>2</sub>; unstressed control) (Fig. 3b). Endogenous hRad9 was distributed to both cytoplasm and nucleus of untreated cells (Fig. 3c). A few sites of co-localization of c-myc-hOGG1 and endogenous hRad9 were observed in nucleus of control

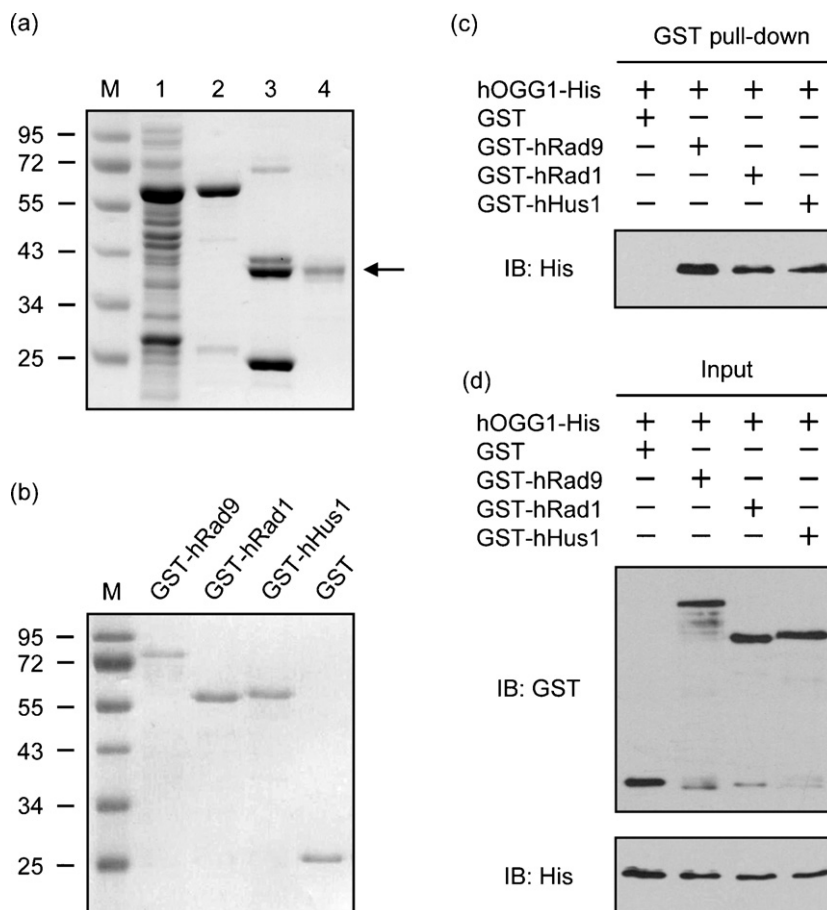


**Fig. 2.** hOGG1-His, GST-fused hRad9, hRad1, and hHus1 were purified with a bacterial expression system, and the physical interactions between purified proteins were analyzed with GST pull-down assays. (a) GST-hOGG1-His was bacterially expressed and purified by affinity chromatography using glutathione-Sepharose 4B and Ni-NTA agarose resins. To evaluate the purity and estimate the molecular weight of the proteins, the product of each step was analyzed by SDS-PAGE and Coomassie brilliant blue staining. The arrow indicates the purified hOGG1-His protein. M, molecular size marker: (1) soluble extracts of cells harboring GST-hOGG1-His; (2) GST-hOGG1-His fraction obtained from affinity chromatography using glutathione-Sepharose 4B resin; (3) protein fractions after thrombin treatment; (4) hOGG1-His fraction purified by affinity chromatography using Ni-NTA agarose resin. (b) GST-fused hRad9, hRad1, and hHus1 were bacterially expressed and purified by affinity chromatography using glutathione-Sepharose 4B and Ni-NTA agarose resins. Purified proteins were analyzed by SDS-PAGE and Coomassie brilliant blue staining. (c) One microgram of GST-fused hRad9, hRad1, hHus1, or GST was immobilized on glutathione-Sepharose 4B resin and incubated with 1  $\mu$ g of hOGG1-His. The pulled down pellets were resolved using SDS polyacrylamide gel and detected by Western blot analysis using anti-His. (d) Input proteins used in (c) GST pull-down experiment were determined with SDS-PAGE followed by Western blot analysis using anti-GST or anti-His.

cells (Fig. 3d). In  $H_2O_2$ -treated cells, most of c-myc-hOGG1 and endogenous hRad9 were distributed throughout the nucleus, with occasional clusters (Fig. 3f and g). The majority of the nuclear c-myc-hOGG1 signal overlapped with the endogenous hRad9 signal, suggesting hOGG1 and the human 9-1-1 complex occupies some common sites following DNA damage.

### 3.3. hRad9, hRad1 and hHus1 enhanced the glycosylase activity of hOGG1

In order to determine whether hRad9, hRad1, or hHus1 altered the DNA glycosylase activity of hOGG1, we added purified GST-hRad9, GST-hRad1 or GST-hHus1 (20 pmol) to increasing doses (5, 10, 20 pmol) of purified hOGG1-His in the presence of a radiolabeled DNA duplex containing an 8-oxoG/C mismatch (Fig. 4). As the concentration of hOGG1-His increased, the amount of cleaved oligonucleotide also increased in a dose-dependent manner. Adding GST alone did not affect the activity of hOGG1 (Fig. 4c). hOGG1 glycosylase activity was enhanced by the presence of GST-hRad9, GST-hRad1, or GST-hHus1 (Fig. 4a, lanes 6–8, 10–12, and 14–16). When 5 pmol of hOGG1-His was reacted with 20 pmol of GST-hRad9, GST-hRad1, or hHus1, hOGG1 activity was increased 3.4, 3.3 or 2.9 times, respectively. Incubating radiolabeled DNA duplexes containing an 8-oxoG/C mismatch with GST-hRad9, GST-hRad1, or GST-hHus1 alone (without hOGG1) did not produce cleaved products (Fig. 4a, lanes 5, 9, and 13). We also combined hOGG1-His (20 pmol) with all the three subunits of the human 9-1-1 complex (20 pmol each of GST-hRad9, GST-hRad1 and GST-hHus1) and observed its effect on the 8-oxoG/C mismatch DNA (Fig. 4d and e). GST was used to keep the overall protein concentration identical for

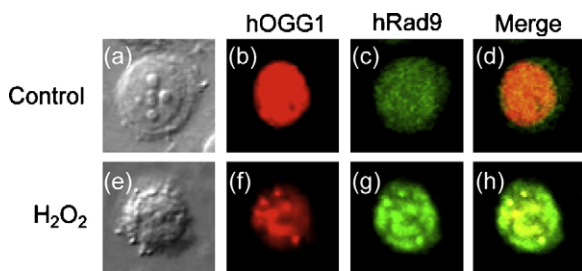


**Fig. 3.** Co-localization of hOGG1 with hRad9 following  $H_2O_2$  treatment. HEK293 cells were transiently transfected with c-myc-hOGG1 expressing vector. After 24 h incubation, cells were treated with 5 mM  $H_2O_2$  for 1 h (e–h). The cells were stained with Alexa Fluor 647-conjugated mouse anti-c-myc (red, b and f) and polyclonal anti-hRad9 followed with FITC-conjugated anti-rabbit IgG (blue, c and g). (a) and (e) are the cell images. (d) and (h) are the merged images of (b)/(c) and (f)/(g), respectively.

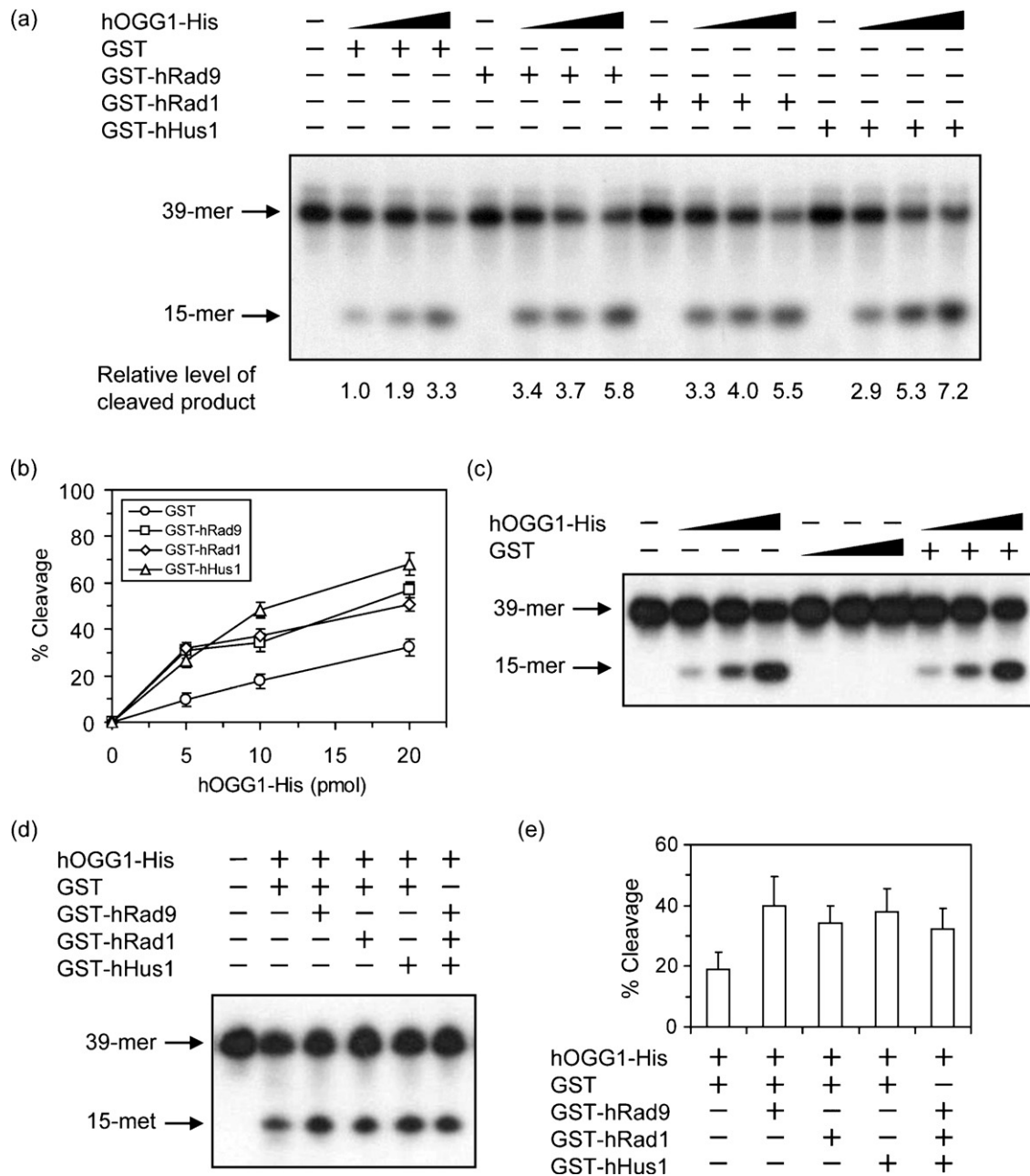


**Fig. 4.** hRad9, hRad1, and hHus1 stimulated hOGG1 activity. (a) Purified hOGG1-His (5, 10, or 20 pmol) and GST-fused hRad9, hRad1, and hHus1 (20 pmol/subunit) were reacted with 1 pmol of 5'-end-labeled 39-mer oligonucleotide duplexes containing an 8-oxoG/C mismatch. After 1 h incubation at 37 °C, the cleavage products were analyzed using 18% denaturing polyacrylamide gel electrophoresis and a BAS2000 image analyzer. (c) 5'-end-labeled 39-mer oligonucleotide duplexes containing 8-oxoG/C mismatch were reacted with the mixtures of purified hOGG1-His (5, 10, 20 pmol) and GST (20 pmol) or GST (5, 10, 20 pmol) alone for 1 h at 37 °C. (d) Purified hOGG1-His (20 pmol) and GST, GST-fused hRad9, hRad1, or hHus1 (20 pmol) were reacted with 1 pmol of 5'-end-labeled 39-mer oligonucleotide duplexes containing an 8-oxoG/C mismatch. After 1 h incubation at 37 °C, the cleavage products were analyzed. (b and e) Cleavage products obtained from three independent experiments of (a) and (d) were quantified, estimated as % cleavage and plotted with the diagram.

all reactions. Incubation of hOGG1-His with all the three subunits of the human 9–1–1 complex mediated only a 1.7-fold increase in hOGG1 activity, which was less than increases mediated by individual subunits of the 9–1–1 complex (1.8- to 2.1-fold increases). Taken together, these results demonstrated that human 9–1–1 enhanced the *in vitro* 8-oxoG excision activity of hOGG1.

#### 3.4. hRad9, hRad1, and hHus1 enhanced the DNA binding activity of hOGG1

Sodium borohydride (NaBH<sub>4</sub>) that traps the enzyme in the form of a covalently bound enzyme–DNA complex [31,32] was treated

with hOGG1-His and the radiolabeled DNA duplex containing 8-oxoG/C to determine the effect of hRad9, hRad1, and hHus1 on the DNA binding activity of hOGG1. As shown in Fig. 5a, NaBH<sub>4</sub> treatment resulted in the formation of hOGG1-His and 8-oxoG/C duplex complexes (lane 2). No trapped complexes were observed when we conducted the trapping assay without hOGG1, i.e., using GST, GST-hRad9, GST-hRad1, or GST-hHus1 by themselves in the reaction with the duplexes (lanes 3–6). In contrast, when we incubated hOGG1-His together with GST-hRad9, GST-hRad1, or GST-hHus1, trapped complexes comprised of covalently linked hOGG1-His and 8-oxoG/C duplex increased 2.2-, 2.0-, or 2.8-fold, respectively (Fig. 5b lanes 4–6). We achieved a 2.6-fold increase in trapped com-

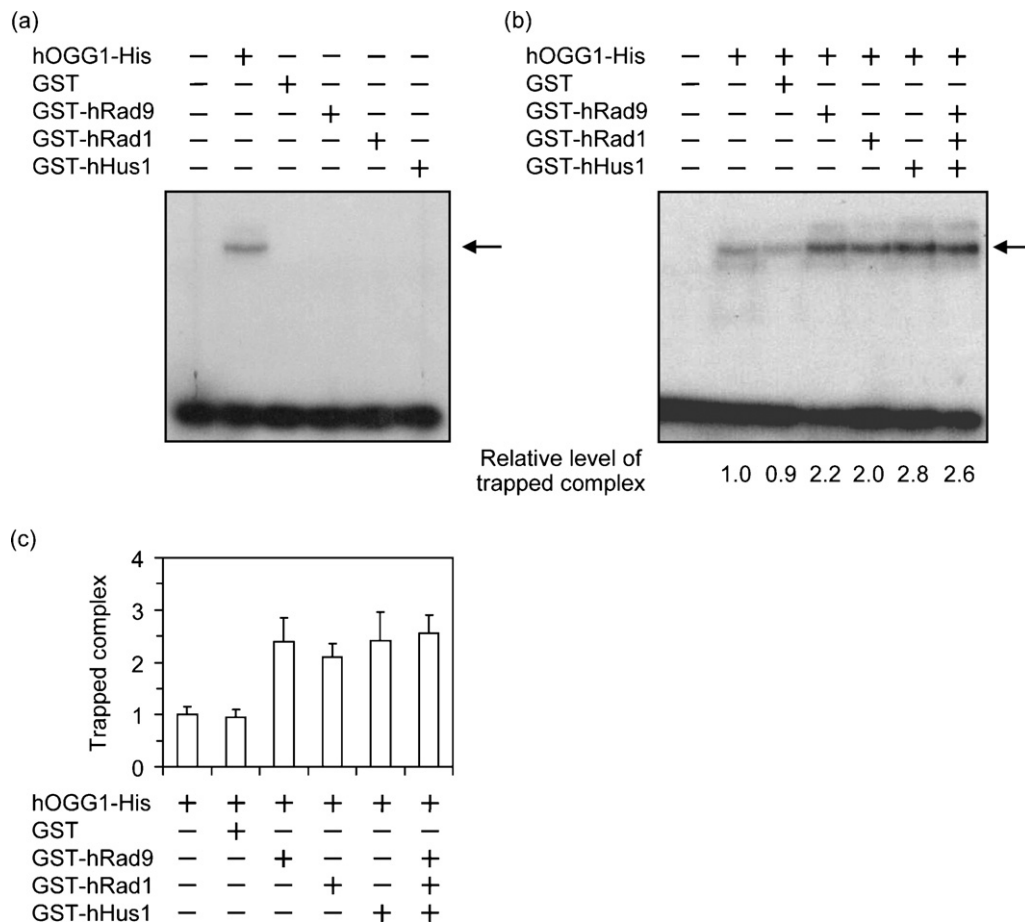


**Fig. 5.** hRad9, hRad1, and hHus1 enhanced the DNA binding activity of hOGG1. (a and b) Purified hOGG1-His, GST, GST-fused hRad9, hRad1, and hHus1 (20 pmol) were mixed and incubated for 30 min with 1 pmol of 5'-end-labeled 39-mer oligonucleotide duplexes containing an 8-oxoG/C mismatch in the presence of 50 mM NaBH<sub>4</sub>. Reactions were terminated with 5× SDS polyacrylamide gel loading buffer, resolved on 12% SDS polyacrylamide gel, and analyzed with a BAS2000 image analyzer. Arrows indicate the trapped complexes containing hOGG1-His and its DNA substrate. (c) Trapped hOGG1-His and DNA substrate complexes from three independent assays were quantified using a BAS2000 image analyzer and the average and standard deviation (error bars) were plotted as a bar diagram. An average level of hOGG1-His-DNA trapped complex was estimated as 1.

plexes by incubating hOGG1-His with all the three of the human 9-1-1 complex subunits (GST-hRad9, GST-hRad1, and GST-hHus1; lane 7), similar to the results we observed when incubating hOGG1-His and individual human 9-1-1 components. This result suggested that human 9-1-1 enhanced the DNA binding activity of hOGG1.

**3.5. Individual human 9-1-1 subunits and trimeric human 9-1-1 complex showed similar activities to enhance in vitro hOGG1 glycosylase activity**

To express and purify 9-1-1 complex, *E. coli* cell expressing all subunits of 9-1-1 complex was established by co-transformation with expression vectors containing hRad9 (polyhistidine-untagged hRad9), His-hRad1 and His-hHus1 genes. The expression of 9-1-1 was induced in selected cell and verified with SDS-PAGE followed by Coomassie brilliant blue staining (data not shown). The purification of His-tagged proteins (hRad1 and hHus1) was performed with affinity chromatography using Ni-NTA agarose resin. Elutes were applied to Superdex 200 (10/30GL) gel filtration column. The elute fractions obtained from size fractionations by gel filtration were verified with SDS-PAGE followed by Coomassie brilliant blue staining (Fig. 6a). The elute fractions 11–18 contained His-untagged hRad9 as well as His-tagged hRad1 and hHus1. His-untagged hRad9 could be purified by affinity chromatography using Ni-NTA agarose resin and hRad9, His-hRad1 and His-hHus1 presented in the same elute fractions of gel filtration chromatography. This means that

hRad9, His-hRad1 and His-hHus1 simultaneously expressed in *E. coli* cell interacted with each other and could be purified as a trimeric 9-1-1 complex. His-tagged hRad9, hRad1 and hHus1 were also purified from *E. coli* cells separately transformed with His-hRad9, hRad1, hHus1 expressing vectors (Fig. 6b). hOGG1-His (20 pmol) was combined with His-hRad9, His-hRad1, His-hHus1, and a trimeric 9-1-1 complex (20 pmol each) and hOGG1 glycosylase activity assay was performed (Fig. 6c and d). hOGG1 activity was enhanced by the addition of His-hRad9, His-hRad1, His-hHus1 and a trimeric 9-1-1 complex in reaction mixtures. Incubation of hOGG1-His with a trimeric 9-1-1 complex mediated a 4-fold increase in hOGG1 activity, which was almost the same with those obtained in incubations of hOGG1-His and individual subunits of the 9-1-1 (3.8- to 3.9-fold increase).

**3.6. Over-expression of human 9-1-1 subunits reduced H<sub>2</sub>O<sub>2</sub>-induced 8-oxoG lesions**

To investigate whether the human 9-1-1-mediated increase in hOGG1 activity was sufficient to decrease levels of DNA damage in cells undergoing oxidative stress, we measured *in vivo* levels of 8-oxoG residues in HEK293 cells transiently expressing hOGG1 or human 9-1-1 under ROS generating conditions. We treated transiently transfected cells with a ROS generating agent, H<sub>2</sub>O<sub>2</sub>, for 1 h to mediate the formation of 8-oxoG lesions. We stained cells with a FITC-conjugated probe that binds to 8-oxoG lesions,

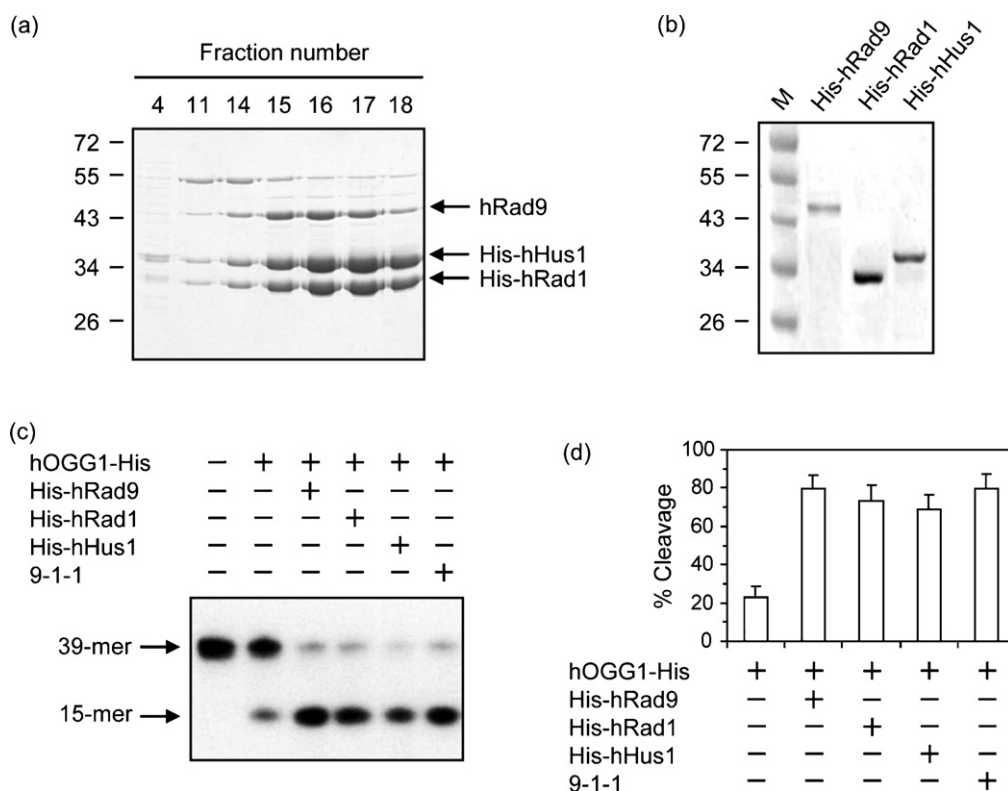


**Fig. 6.** Individual or a trimeric 9–1–1 complex showed a similar hOGG1 stimulation activity. (a) hRad9, His-hRad1 and His-hHus1 were expressed in *E. coli* cell co-transformed with hRad9, His-hRad1 and His-hHus1 expressing vectors and purified with affinity chromatography using Ni-NTA agarose resin. Elutes containing hRad9, His-hRad1 and His-hHus1 were subjected to gel filtration chromatography using Superdex 200 (10/30GL) column. The elute fractions obtained from gel filtration chromatography were analyzed with SDS-PAGE followed by Coomassie brilliant blue staining. (b) His-hRad9, His-hRad1 or His-hHus1 was separately expressed in *E. coli* cells and purified with affinity chromatography using Ni-NTA agarose resin. Purified His-hRad9, His-hRad1 and His-hHus1 were analyzed with SDS-PAGE followed by Coomassie brilliant blue staining. M means a molecular size marker. (c) Purified hOGG1-His (20 pmol), His-hRad9, His-hRad1, His-hHus1 and a trimeric 9–1–1 complex (20 pmol each) were reacted with 1 pmol of 5'-end-labeled 39-mer oligonucleotide duplexes containing an 8-oxoG/C mismatch. After 1 h incubation at 37 °C, the cleavage products were analyzed using 18% denaturing polyacrylamide gel electrophoresis and a BAS2000 image analyzer. (d) Cleavage products obtained from three independent experiments of (c) were quantified, estimated as % cleavage and plotted with the diagram.

and we analyzed 8-oxoG residues in H<sub>2</sub>O<sub>2</sub>-treated cells using a flow cytometry (Fig. 7). H<sub>2</sub>O<sub>2</sub> treatment increased the FITC fluorescence (Fig. 7a, black solid line), but transient over-expression of hOGG1 or individual components of human 9–1–1 decreased this H<sub>2</sub>O<sub>2</sub>-induced FITC fluorescence (Fig. 7a–d, red solid lines). Co-expression of all the three subunits of the human 9–1–1 complex yielded a greater reduction in FITC fluorescence than expression of isolated individual 9–1–1 components (Fig. 7e, red solid line). In fact, over-expression of hOGG1 and all the three subunits of human 9–1–1 mediated the greatest reduction in FITC fluorescence that we observed herein (Fig. 7f and g, red solid lines). The reduction in H<sub>2</sub>O<sub>2</sub>-mediated FITC fluorescence was least to greatest under the following expression conditions: all the three subunits of human 9–1–1 but no hOGG1, hOGG1 but no 9–1–1 components, and hOGG1 together with all subunits of human 9–1–1 (Fig. 7g red dotted line, black dotted line, and red solid line).

The reduction of H<sub>2</sub>O<sub>2</sub>-induced 8-oxoG residues in hOGG1 and human 9–1–1 proteins expressed HEK293 cells was further determined with spectrofluorometric analysis for a statistical analysis of multiple independent experiments (Fig. 8). Over-expression of hOGG1 or all the three subunit of human 9–1–1 reduced the FITC fluorescence intensity by 30% or 20%, respectively, which was higher than those obtained from over-expression of individual subunits (6–8% reduction). When hOGG1 was co-expressed with all subunits of human 9–1–1 proteins, FITC fluorescence intensity was reduced by 43%. These results suggested that individual components of human 9–1–1 might have slightly enhanced the 8-oxoG excision activity of hOGG1

in H<sub>2</sub>O<sub>2</sub>-treated cells, but the greatest effect was derived from the entire human 9–1–1 complex.

#### 4. Discussion

Cells repair oxidatively damaged DNA lesions mainly through the BER pathway, which is tightly coupled with the cell cycle regulation and DNA damage checkpoint systems. Together, these systems function to preserve genome integrity and prevent carcinogenesis by monitoring the cellular damage state [33–35]. Human 9–1–1 complexes recognize DNA damage and are loaded onto DNA by Rad17/RFC2–5, an alternative complex of Rad17/RFC, to form DNA damage-responsive complexes; these complexes then transduce the damage signal to downstream effectors [16,36,37]. The human 9–1–1 complex is a proposed component of the BER pathway, because it interacts with several BER-related proteins (APE1, Pol β, FEN1, and DNA ligase I) to enhance DNA repair activities [22–26]. The human 9–1–1 also interacts with several BER DNA glycosylases (MYH, NEIL1, and TDG) to enhance their activity [28–30]. In our preliminary work, we investigated interactions between hRad9 and BER DNA glycosylases using co-immunoprecipitation in transiently transfected HEK293 cells. We identified a novel interaction between hRad9 and hOGG1 (data not shown).

In this work, we investigated the effect that human 9–1–1 had on hOGG1 activities, in addition to studying the physical interaction between them. In co-immunoprecipitation experiments using transiently transfected HEK293 cells, hOGG1 interacted with hRad9, hRad1, and hHus1 as individual proteins (Fig. 1a). hOGG1 was

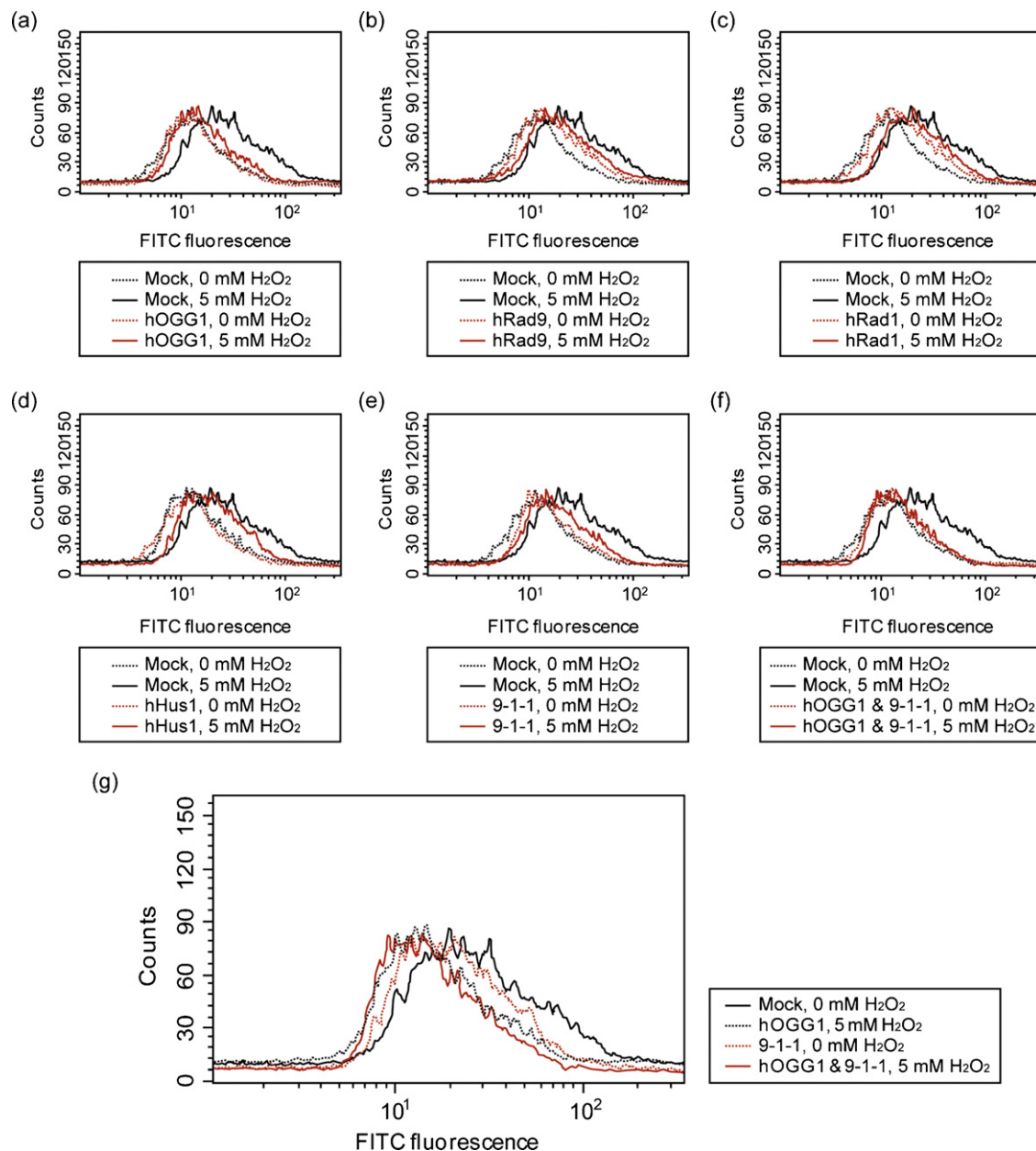


**Fig. 7.** Flow cytometric analysis showed that the over-expression of hOGG1 and human 9-1-1 reduced the number of H<sub>2</sub>O<sub>2</sub>-induced 8-oxoG residues in cells. HEK293 cells transfected with hOGG1, hRad9, hRad1, or hHus1 expressing vector were incubated for 24 h and treated with 5 mM H<sub>2</sub>O<sub>2</sub> for 1 h. After fixation, the cells were treated with a FITC-conjugated 8-oxoG detection probe. FITC fluorescence was analyzed with a flow cytometer. Mock means the sample transfected with the empty parental vector, pCMV Tag3A.

shown to interact with the phosphorylated form of hRad9, not the hyperphosphorylated form. The hRad9 contains several phosphorylation sites and exogenously over-expressed hRad9 has been known to appear as several bands of different sizes in mammalian cells, including HEK293 cells. hRad9 phosphorylation is most likely the mechanism by which hRad9 is differently regulated in response to DNA damage and cell cycle regulation [38,39]. A recent study reported that the interaction of the 9-1-1 complex with the BRCT I-II region of TopBP1, an activator of ATR-ATRIP complex generated in response to incompletely replicated or damaged DNA, is necessary in order for ATR-ATRIP to bind to the ATR-activating domain of TopBP1. This interaction between the 9-1-1 complex and TopBP1 depends on the phosphorylation of hRad9 at Ser387 [21], which is constitutively phosphorylated [39]. However, the function of the hyperphosphorylated-hRad9, which is induced by the phosphorylation of Ser272 and Thr292 residues in response

to ionizing radiation (IR) and mitotic signals [39], is inaccurate. Although it is not clear why the interaction between hOGG1 and the hyperphosphorylated-hRad9 was not observed, the interaction between hOGG1 and hRad9 may be regulated by the status of phosphorylated-hRad9.

We further confirmed the physical interaction between hOGG1 and human 9-1-1 using GST pull-down assays with purified hOGG1-His, GST-fused hRad9, hRad1, and hHus1 (Fig. 2c). In previous studies concerning other BER components, MYH interacted with the 9-1-1 complex mainly via the hHus1 subunit [28]. In contrast, the present studies showed that hOGG1 possessed equivalent affinities for hRad9, hRad1, and hHus1, a result similar to that obtained for TDG and NEIL1 [29,30]. These variable subunit affinities for different DNA glycosylases have been suggested that different BER pathways regulate the 9-1-1 complex in response to different DNA damage signals [30].

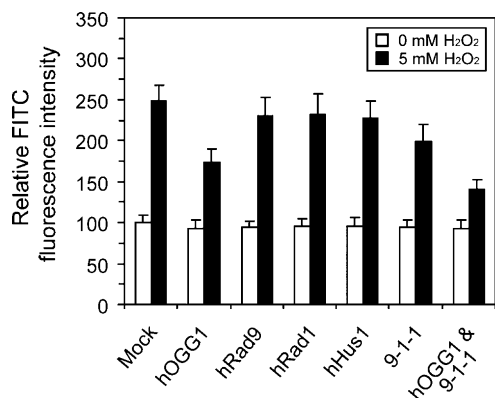


**Fig. 8.** The reductions of H<sub>2</sub>O<sub>2</sub>-induced 8-oxoG residues in hOGG1 or human 9–1–1 over-expressed HEK293 cells were determined with spectrofluorometric analysis. HEK293 cells transfected with hOGG1, hRad9, hRad1, or hHus1 expressing vectors were incubated for 24 h and treated with 5 mM H<sub>2</sub>O<sub>2</sub> for 1 h. After fixation, cells were treated with a FITC-conjugated 8-oxoG detection probe. FITC fluorescence was measured using a spectrofluorometer (Geminin EM, Molecular Devices, USA) with excitation at 495 nm and emission at 515 nm. FITC fluorescences obtained from three independent experiments were quantified and plotted with the diagram. FITC fluorescence obtained from Mock (H<sub>2</sub>O<sub>2</sub>-untreated HEK293 cells) was estimated as 100.

H<sub>2</sub>O<sub>2</sub> treatment enhanced co-localization of c-myc-hOGG1 and endogenous hRad9 in the nucleus of transiently transfected HEK 293 cells, suggesting that hOGG1 and human 9–1–1 accumulated in repair foci after DNA damage (Fig. 3 and Supplementary data 1 and 2). The hOGG1 protein has two specific enzymatic activities during its function as a DNA glycosylase: it excises 8-oxoG, and it generates strand cleavage 3' to the AP site by  $\beta$ -elimination. These functions could be enhanced by each of the individual 9–1–1 subunits (Fig. 4a); in contrast, MYH is stimulated only by hHus1 [28]. We confirmed stimulations of hOGG1 glycosylase activity by hRad9, hRad1, or hHus1 in our trapping assay using NaBH<sub>4</sub>. Accumulation of covalent complexes between hOGG1 and the 8-oxoG/C mismatched duplexes in the presence of hRad9, hRad1, or hHus1 suggested that human 9–1–1 enhanced the hOGG1 DNA binding activity (Fig. 5).

Incubating hOGG1 with all the three subunits of the human 9–1–1 complex enhanced the DNA glycosylase and DNA binding activities of hOGG1, but the effects were less than those obtained from incubation with the individual subunits (Figs. 4d and 5). One explanation for these results lies in our using bacterially expressed fusion proteins for these assays. It is possible that the physical and functional interactions between bacterially expressed and His-tagged hOGG1 and GST-tagged human 9–1–1 proteins did not perfectly replicate *in vivo* interactions. Although hRad9, hRad1, and hHus1 purified from a bacterial expression system can form a trimeric protein complex [40], we think that GST-fused hRad9, hRad1, and hHus1 possess a reduced ability to make a trimeric 9–1–1 complex. As such, co-incubation with all the three subunits of 9–1–1 complex did not mediate a stronger effect than treatment with any of the individual subunits. Thus, we established an *E. coli* cell simultaneously expressing all the three subunits (His-untagged hRad9, His-tagged hRad1 and His-tagged hHus1) to form and purify a trimeric 9–1–1 complex. His-untagged hRad9 could be purified by affinity chromatography using Ni-NTA agarose resin and hRad9, His-hRad1 and His-hHus1 were shown to present in the same elute fractions of gel filtration chromatography (Fig. 6a). This strongly indicates that a trimeric 9–1–1 complex is successfully formed and purified in an *E. coli* cell simultaneously expressing hRad9, His-hRad1 and His-hHus1. Incubation of hOGG1 and a trimeric 9–1–1 complex enhanced the hOGG1 activity by four times. However, this was almost the same value with those obtained in incubations of

hOGG1 and individual subunits of the 9–1–1 complex (Fig. 6c and d). Nonetheless, our findings strongly supported that hOGG1 interacts physically and functionally with the human 9–1–1 complex, as previously demonstrated in other BER proteins, namely TDG and NEIL1, which interacted with trimeric human 9–1–1 complexes purified from yeast or insect cell-baculovirus expression systems [29,30].

The dramatic reductions in H<sub>2</sub>O<sub>2</sub>-induced 8-oxoG residues in cells over-expressing hOGG1, hRad9, hRad1, and hHus1 were observed in flow cytometric and spectrofluorometric analysis (Figs. 7 and 8), which suggested that human 9–1–1 stimulated the removal of 8-oxoG generated by H<sub>2</sub>O<sub>2</sub> in these cells. Over-expression of all the three subunits of human 9–1–1 reduced FITC fluorescence more than over-expression of individuals (Figs. 7e, red solid line and 8). The reduction of FITC fluorescence in H<sub>2</sub>O<sub>2</sub>-treated cells was maximal when hOGG1 and all the three subunits of human 9–1–1 were co-expressed (Fig. 7g, red solid line and 8). Also, in the statistical analysis using spectrofluorometer, over-expression of hOGG1 or all the three subunits of human 9–1–1 reduced the FITC fluorescence intensity by 30% or 20%, respectively. When hOGG1 was co-expressed with all subunits of human 9–1–1 proteins, FITC fluorescence intensity was reduced by 43%. However, co-expression of individual 9–1–1 proteins and hOGG1 did not further decrease the H<sub>2</sub>O<sub>2</sub>-induced FITC fluorescence, compared with that of cells expressing only hOGG1 (data not shown). These results strongly demonstrate that the human 9–1–1 complex as a whole mediated the most effective stimulation of 8-oxoG-removing activity of hOGG1 in H<sub>2</sub>O<sub>2</sub>-treated cells.

DNA ligases I and III are involved in the long- and short-patch BER pathways, respectively [26]. Previous work has suggested that the 9–1–1 complex is mainly involved in the long-patch BER pathway, because the 9–1–1 complex interacted with DNA ligase I but not DNA ligase III. In contrast, the human 9–1–1 complex physically and functionally interacted with NEIL1, a component of the non-replicative short-patch BER pathway [29]. Herein, the human 9–1–1 complex interacted with hOGG1 and enhanced its activity. Previously, hOGG1 has been implicated in both the non-replicative short-patch BER and the replication-associated long-patch BER pathway, a repair mode activated when lesions persist or are formed at replication [41–43]. Specifically, when 8-oxoG residues are present in non-replicating DNA, hOGG1 is involved in the Pol  $\beta$ -dependent short-patch BER. However, when 8-oxoG residues are formed at or near a replication fork, the replication-associated long-patch BER pathway is the preferred repair mode [42]. The removal of adenine from the 8-oxoG/A mismatch, generated while replicating DNA strands containing 8-oxoG/C mismatch, is repaired by the BER glycosylase MYH. This correction leads to the formation of 8-oxoG/C mismatches, which are in turn corrected by hOGG1-mediated BER. Although our results do not clarify whether the 9–1–1 complex is directly involved in short-patch BER, the 9–1–1 complex might be a component of both the short-patch and the long-patch BER that repairs DNA lesions produced during replication.

#### Conflict of interest

The authors declare that there are no conflicts of interest.

#### Acknowledgements

This work was supported by National Research Laboratory Program (M10400000046-04J0000-04610), the Korea Research Foundation (KRF-2006-005-J03403), the Real Time Molecular Imaging Project of the Korea Ministry of Science and Technology, and WCU (World Class University, R33-2008-000-1071) program through the Korea Science and Engineering Foundation funded by

the Ministry of Education, Science and Technology. We thank Dr. Darrick S.H.L. Kim (CurXcel Corp.) for helpful comments on the manuscript.

## Appendix A. Supplementary data

Supplementary data associated with this article can be found at doi:10.1016/j.dnarep.2009.06.004.

## References

- [1] T. Lindahl, Instability and decay of the primary structure of DNA, *Nature* 362 (1993) 709–715.
- [2] A.P. Breen, J.A. Murphy, Reactions of oxyl radicals with DNA, *Free Radic. Biol. Med.* 18 (1995) 1033–1077.
- [3] H. Wiseman, H. Kaur, B. Halliwell, DNA damage and cancer: measurement and mechanism, *Cancer Lett.* 93 (1995) 113–120.
- [4] K.B. Beckman, B.N. Ames, Oxidative decay of DNA, *J. Biol. Chem.* 272 (1997) 19633–19636.
- [5] M.K. Shigenaga, E.N. Aboujaoude, Q. Chen, B.N. Ames, Assays of oxidative DNA damage biomarkers 8-oxo-2'-deoxyguanosine and 8-oxoguanine in nuclear DNA and biological fluids by high-performance liquid chromatography with electrochemical detection, *Methods Enzymol.* 234 (1994) 16–33.
- [6] T. Melvin, S.M.T. Cunniff, P. O'Neill, A.W. Parker, T. Roldan-Arjona, Guanine is the target for direct ionization of damage in DNA, as detected using excision enzymes, *Nucleic Acids Res.* 21 (1998) 4935–4942.
- [7] H.E. Krokan, H. Nilsen, F. Skorpen, M. Otterlei, G. Slupphaug, Base excision repair of DNA in mammalian cells, *FEBS Lett.* 476 (2000) 73–77.
- [8] S. Mitra, T.K. Hazra, R. Roy, S. Ikeda, T. Biswas, J. Lock, I. Boldogh, T. Izumi, Complexities of DNA base excision repair in mammalian cells, *Mol. Cells* 7 (2002) 305–312.
- [9] T.K. Hazra, A. Das, S. Das, S. Choudhury, Y.W. Kow, R. Roy, Oxidative DNA damage repair in mammalian cells: a new perspective, *DNA Repair* 6 (2007) 470–480.
- [10] S.S. David, V.L. O'Shea, S. Kunda, Base-excision repair of oxidative DNA damage, *Nature* 447 (2007) 941–950.
- [11] H. Aburatani, Y. Hippo, T. Ishida, R. Takashima, C. Matsuba, T. Kodama, M. Takao, A. Yasui, K. Yamamoto, M. Asano, K. Fukasawa, T. Yoshinari, H. Inoue, E. Ohtsuka, S. Nishimura, Cloning and characterization of mammalian 8-hydroxyguanine-specific DNA glycosylase/apurinic, apyrimidinic lyase, a functional mutM homologue, *Cancer Res.* 57 (1997) 2151–2156.
- [12] S. Nishimura, Involvement of mammalian OGG1 (MMH) in excision of the 8-hydroxyguanine residue in DNA, *Free Radic. Biol. Med.* 32 (2002) 813–821.
- [13] Y. Nakabeppu, D. Tsuchimoto, A. Ichinoe, M. Ohno, Y. Ide, S. Hirano, D. Yoshimura, Y. Tominaga, M. Furuichi, K. Sakumi, Biological significance of the defense mechanisms against oxidative damage in nucleic acids caused by reactive oxygen species: from mitochondria to nuclei, *Ann. N. Y. Acad. Sci.* 1011 (2004) 101–111.
- [14] S. Boiteux, J.P. Radicella, The human OGG1 gene: structure, functions and its implication in the process of carcinogenesis, *Arch. Biochem. Biophys.* 377 (2000) 1–8.
- [15] S.H. Willson, T.A. Kunkel, Passing the baton in base excision repair, *Nat. Struct. Biol.* 7 (2000) 176–178.
- [16] C. Venclovas, M.P. Thelen, Structure-based predictions of Rad1, Rad9, Hus1 and Rad17 participation in sliding clamp and clamp-loading complexes, *Nucleic Acids Res.* 28 (2000) 2481–2493.
- [17] L. Zou, D. Cortez, S.J. Elledge, Regulation of ATR substrate selection by Rad17-dependent loading of Rad9 complexes onto chromatin, *Genes Dev.* 16 (2002) 198–208.
- [18] Q. Liu, S. Guntuku, X.S. Cui, S. Matsuoka, D. Cortez, K. Tamai, G. Luo, S. Carattini-Rivera, F. DeMayo, A. Bradley, L.A. Donehower, S.J. Elledge, Chk1 is an essential kinase that is regulated by Atr and required for the G(2)/M DNA damage checkpoint, *Genes Dev.* 14 (2000) 1448–1459.
- [19] S. Bao, T. Lu, X. Wang, H. Zheng, L.E. Wang, Q. Wei, W.N. Hittelman, L. Li, Disruption of the Rad9/Rad1/Hus1 (9–1–1) complex leads to checkpoint signaling and replication defects, *Oncogene* 23 (2004) 5586–5593.
- [20] S. Delacroix, J.M. Wagner, M. Kobayashi, K. Yamamoto, L.M. Karnitz, The Rad9–Hus1–Rad1 (9–1–1) clamp activates checkpoint signaling via TopBP1, *Genes Dev.* 21 (2007) 1472–1477.
- [21] J. Lee, A. Kumagai, W.G. Dunphy, The Rad9–Hus1–Rad1 checkpoint clamp regulates interaction of TopBP1 with ATR, *J. Biol. Chem.* 282 (2007) 28036–28044.
- [22] A. Gembka, M. Toueille, E. Smirnova, R. Polt, E. Ferrari, G. Villani, U. Hubscher, The checkpoint clamp, Rad9–Rad1–Hus1 complex, preferentially stimulates the activity of apurinic/apyrimidinic endonuclease 1 and DNA polymerase beta in long patch base excision repair, *Nucleic Acids Res.* 35 (2007) 2596–2608.
- [23] W. Wang, P. Brandt, M.L. Rossi, L. Lindsey-Boltz, V. Podust, E. Fanning, A. Sancar, R.A. Bambara, The human Rad9–Rad1–Hus1 checkpoint complex stimulates flap endonuclease 1, *Proc. Natl. Acad. Sci. U.S.A.* 101 (2004) 16762–16767.
- [24] E. Friedrich-Heineken, M. Toueille, B. Tannler, C. Burki, E. Ferrari, M.O. Hottiger, U. Hubscher, The two DNA clamps Rad9/Rad1/Hus1 complex and proliferating cell nuclear antigen differentially relate flap endonuclease I activity, *J. Mol. Biol.* 353 (2005) 980–989.
- [25] M. Toueille, N. El-Andaloussi, I. Frouin, R. Freire, D. Funk, I. Shevelev, E. Friedrich-Heineken, G. Villani, M.O. Hottiger, U. Hubscher, The human Rad9/Rad1/Hus1 damage sensor clamp interacts with DNA polymerase beta and increases its DNA substrate utilization efficiency: implications for DNA repair, *Nucleic Acid Res.* 32 (2004) 3316–3324.
- [26] E. Smirnova, M. Toueille, E. Markkanen, U. Hubscher, The human checkpoint sensor and alternative DNA clamp Rad9–Rad1–Hus1 modulates the activity of DNA ligase I, a component of the long-patch base excision repair machinery, *Biochem. J.* 389 (2005) 13–17.
- [27] D.Y. Chang, A.L. Lu, Interaction of checkpoint proteins Hus1/Rad1/Rad9 with DNA base excision repair enzyme MutY homolog in fission yeast, *Schizosaccharomyces pombe*, *J. Biol. Chem.* 280 (2005) 408–417.
- [28] G. Shi, D.-Y. Chang, C.C. Cheng, X. Guan, C. Venclovas, A.L. Lu, Physical and functional interactions between MutY homolog (MYH) and checkpoint proteins Rad9–Rad1–Hus1, *Biochem. J.* 400 (2006) 53–62.
- [29] X. Guan, H. Bai, G. Shi, A.L. Lu, The human checkpoint sensor Rad9–Rad1–Hus1 interacts with and stimulates NEIL1 glycosylase, *Nucleic Acids Res.* 35 (2007) 2463–2472.
- [30] X. Guan, A. Madabushi, D.Y. Chang, A.L. Lu, The human checkpoint sensor Rad9–Rad1–Hus1 interacts with and stimulates DNA repair enzyme TDG glycosylase, *Nucleic Acids Res.* 35 (2007) 6207–6218.
- [31] H.M. Nash, S.D. Bruerner, O.D. Scharer, T. Kawate, T.A. Addona, E. Spooner, W.S. Lane, G.L. Verdine, Cloning of a yeast 8-oxoguanine DNA glycosylase reveals the existence of a base-excision DNA repair protein superfamily, *Curr. Biol.* 6 (1996) 968–980.
- [32] J. Tchou, A.P. Grollman, The catalytic mechanism of Fpg protein: evidence for a Schiff base intermediate and amino terminus localization of catalytic site, *J. Biol. Chem.* 270 (1995) 11671–11677.
- [33] P.A. Jeggo, M. Lobrich, Contribution of DNA repair and cell cycle checkpoint arrest to the maintenance of genomic stability, *DNA Repair* 5 (2006) 1192–1198.
- [34] C.E. Canman, Replication checkpoint: preventing mitotic catastrophe, *Curr. Biol.* 11 (2001) 121–124.
- [35] J. Bartek, C. Lukas, J. Lukas, Checking on DNA damage in S phase, *Nat. Rev. Mol. Cell Biol.* 5 (2004) 792–804.
- [36] Y. Shiomi, A. Shinozaki, D. Nakada, K. Sugimoto, J. Usukura, C. Obuse, T. Tsurimoto, Clamp and clamp loader structures of the human checkpoint protein complexes, Rad9–1–1 and Rad17-RFC, *Genes Cells* 7 (2002) 861–868.
- [37] V.P. Bermudez, L.A. Lindsey-Boltz, A.J. Cesare, Y. Maniwa, J.D. Griffith, J. Hurwitz, A. Sancar, Loading of the human 9–1–1 checkpoint complex onto DNA by the checkpoint clamp loader hRad17-replication factor C complex *in vitro*, *Proc. Natl. Acad. Sci. U.S.A.* 100 (2003) 1633–1638.
- [38] P. Roos-Mattjus, K.M. Hopkins, A.J. Oestreich, B.T. Vroman, K.L. Johnson, S. Naylor, H.B. Lieberman, L.M. Karnitz, Phosphorylation of human Rad9 is required for genotoxic-activated checkpoint signaling, *J. Biol. Chem.* 278 (2003) 24428–24437.
- [39] R.P. St-Onge, B.D.A. Besley, J.L. Pelley, S. Davey, A role for the phosphorylation of hRad9 in checkpoint signaling, *J. Biol. Chem.* 278 (2003) 26620–26628.
- [40] V.K. Singh, S. Nurmohamed, S.K. Davey, Z. Jia, Tri-cistronic cloning, overexpression and purification of human Rad9, Rad1, Hus1 protein complex, *Protein Express. Purif.* 54 (2007) 204–211.
- [41] P. Fortini, E. Parlanti, O.M. Sidorkina, J. Laval, E. Dogliotti, The type of DNA glycosylases determines the base excision repair pathway in mammalian cells, *J. Biol. Chem.* 274 (1999) 15230–15236.
- [42] P. Fortini, B. Pascucci, E. Parlanti, M. D'Errico, V. Simonelli, E. Dogliotti, 8-Oxoguanine DNA damage: at the crossroad of alternative repair pathways, *Mutat. Res.* 531 (2003) 127–139.
- [43] G. Dianov, C. Bischoff, J. Piotrowski, V.A. Bohr, Repair pathways for processing of 8-oxoguanine in DNA by mammalian cell extracts, *J. Biol. Chem.* 273 (1998) 33511–33516.